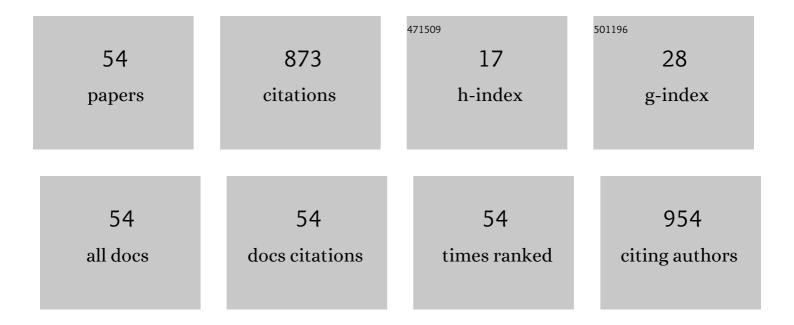
Guillaume Alombert-Goget

List of Publications by Year in descending order

Source: https://exaly.com/author-pdf/1494974/publications.pdf

Version: 2024-02-01



#	Article	IF	CITATIONS
1	Clustering of rare earth in glasses, aluminum effect: experiments and modeling. Journal of Non-Crystalline Solids, 2004, 348, 44-50.	3.1	122
2	Spectroscopic properties of Er3+-doped antimony oxide glass. Journal of Alloys and Compounds, 2014, 603, 132-135.	5.5	54
3	Tb3+/Yb3+ co-activated Silica-Hafnia glass ceramic waveguides. Optical Materials, 2010, 33, 227-230.	3.6	47
4	Up- and down-conversion in Yb3+–Pr3+ co-doped fluoride glasses and glass ceramics. Journal of Non-Crystalline Solids, 2013, 377, 105-109.	3.1	42
5	Rare-earth-activated glass–ceramic waveguides. Optical Materials, 2010, 32, 1644-1647.	3.6	37
6	Highly transparent Nd:Lu2O3 ceramics obtained by coupling slip-casting and spark plasma sintering. Scripta Materialia, 2014, 75, 54-57.	5.2	35
7	Aluminum effect on photoluminescence properties of sol–gel-derived Eu3+-activated silicate glasses. Journal of Non-Crystalline Solids, 2005, 351, 1754-1758.	3.1	33
8	Multilayered YAG-Yb:YAG ceramics: manufacture and laser performance. Journal of Materials Chemistry C, 2014, 2, 10138-10148.	5.5	33
9	Nd3+-doped Lu2O3 transparent sesquioxide ceramics elaborated by the Spark Plasma Sintering (SPS) method. Part 2: First laser output results and comparison with Nd3+-doped Lu2O3 and Nd3+-Y2O3 ceramics elaborated by a conventional method. Optical Materials, 2015, 41, 12-16.	3.6	33
10	Nd3+-doped Lu2O3 transparent sesquioxide ceramics elaborated by the Spark Plasma Sintering (SPS) method. Part 1: Structural, thermal conductivity and spectroscopic characterization. Optical Materials, 2015, 41, 3-11.	3.6	29
11	Rare earth–activated glass-ceramic in planar format. Optical Engineering, 2011, 50, 071105.	1.0	27
12	Bubbles defects distribution in sapphire bulk crystals grown by Czochralski technique. Optical Materials, 2013, 35, 1071-1076.	3.6	27
13	Assignment of Yb 3+ energy levels in the C 2 and C 3i centers of Lu 2 O 3 sesquioxide either as ceramics or as crystal. Journal of Luminescence, 2016, 170, 513-519.	3.1	26
14	Effect of Pulling Rate on Bubbles Distribution in Sapphire Crystals Grown by the Micropulling Down (μ-PD) Technique. Crystal Growth and Design, 2012, 12, 4098-4103.	3.0	23
15	Conjugation of TEM-EDX and optical spectroscopy tools for the localization of Yb ³⁺ , Er ³⁺ and Co ²⁺ dopants in laser glass ceramics composed of MgAl ₂ O ₄ spinel nano-crystals embedded in SiO ₂ glass. Journal of Materials Chemistry C. 2014. 2. 9385-9397.	5.5	21
16	Influence of Nd3+ doping on the structural and near-IR photoluminescence properties of nanostructured TiO2 films. Energy Procedia, 2011, 10, 167-171.	1.8	17
17	Titanium distribution profiles obtained by luminescence and LIBS measurements on Ti: Al 2 O 3 grown by Czochralski and Kyropoulos techniques. Optical Materials, 2017, 65, 28-32.	3.6	17
18	New Er3+ doped antimony oxide based glasses: Thermal analysis, structural and spectral properties. Journal of Alloys and Compounds, 2015, 649, 564-572.	5.5	16

#	Article	IF	CITATIONS
19	Relationship between structure and optical properties in rare earth-doped hafnium and silicon oxides: Modeling and spectroscopic measurements. Journal of Non-Crystalline Solids, 2008, 354, 4719-4722.	3.1	15
20	Qualitative and quantitative bubbles defects analysis in undoped and Ti-doped sapphire crystals grown by Czochralski technique. Optical Materials, 2014, 37, 132-138.	3.6	15
21	Antimony oxide based glasses, novel laser materials. Optical Materials, 2017, 65, 8-14.	3.6	15
22	Pr3+–Yb3+â€codoped lanthanum fluorozirconate glasses and waveguides for visible laser emission. Journal of Non-Crystalline Solids, 2012, 358, 2695-2700.	3.1	13
23	Large Ti-doped sapphire bulk crystal for high power laser applications. Optical Materials, 2014, 36, 2004-2006.	3.6	12
24	Experimental and numerical effects of active afterheater addition on the growth of langatate (La3Ga5.5Ta0.5O14) crystals by the Czochralski method. CrystEngComm, 2018, 20, 1110-1115.	2.6	12
25	Lead-free piezoelectric crystals grown by the micro-pulling down technique in the BaTiO ₃ –CaTiO ₃ –BaZrO ₃ system. CrystEngComm, 2019, 21, 3844-38	85 3 .6	12
26	Large Ti-doped sapphire single crystals grown by the kyropoulos technique for petawatt power laser application. Optical Materials, 2016, 61, 21-24.	3.6	11
27	Luminescence and coloration of undoped and Ti-doped sapphire crystals grown by Czochralski technique. Journal of Luminescence, 2016, 169, 516-519.	3.1	11
28	Spectroscopy of C3i and C2 sites of Nd3+-doped Lu2O3 sesquioxide either as ceramics or crystal. Journal of Luminescence, 2016, 169, 606-611.	3.1	11
29	Frequency converter layers based on terbium and ytterbium activated HfO 2 glass-ceramics. Proceedings of SPIE, 2010, , .	0.8	10
30	Er ³⁺ /Yb ³⁺ /Ce ³⁺ Co-Doped Fluoride Glass Ceramics Waveguides for Application in the 1.5Âμm Telecommunication Window. Advances in Science and Technology, 2010, 71, 16-21.	0.2	9
31	Polycrystalline Yb ³⁺ –Er ³⁺ -co-doped YAG: Fabrication, TEM-EDX characterization, spectroscopic properties, and comparison with the single crystal. Journal of Materials Research, 2014, 29, 2288-2296.	2.6	9
32	Thermo optical coefficient of tin-oxide films measured by ellipsometry. Journal of Applied Physics, 2015, 118, .	2.5	9
33	Interface effect on titanium distribution during Ti-doped sapphire crystals grown by the Kyropoulos method. Optical Materials, 2017, 69, 73-80.	3.6	9
34	Thermal and Optical Characterization of Undoped and Neodymium-Doped Y ₃ ScAl ₄ O ₁₂ Ceramics. Journal of Physical Chemistry C, 2014, 118, 13781-13789.	3.1	7
35	Titanium distribution in Ti-sapphire single crystals grown by Czochralski and Verneuil technique. Optical Materials, 2016, 51, 1-4.	3.6	7
36	Scattering defect in large diameter titanium-doped sapphire crystals grown by the Kyropoulos technique. CrystEngComm, 2018, 20, 412-419.	2.6	7

#	Article	IF	CITATIONS
37	Glass-Ceramic waveguides: Fabrication and properties. , 2010, , .		6
38	Glass-based erbium activated micro-nano photonic structures. , 2009, , .		4
39	Thermally driven dual-frequency Q-switching of Nd:YGd_2Sc_2Al_2GaO_12 ceramic laser. Optics Express, 2014, 22, 10792.	3.4	4
40	Glass-ceramics coating of silica microspheres. , 2009, , .		3
41	Opal-Type Photonic Crystals: Fabrication and Application. Advances in Science and Technology, 0, , .	0.2	3
42	Rare-earth-activated glasses for solar energy conversion. , 2011, , .		3
43	Rare-earth doped materials enhance silicon solar cell efficiency. SPIE Newsroom, 0, , .	0.1	3
44	Erbium-Activated Silica-Hafnia: a Reliable Photonic System. , 2008, , .		2
45	Er3+-activated photonic structures fabricated by sol-gel and rf-sputtering techniques. , 2009, , .		2
46	Down-converter based on rare earth doped fluoride glass to improve Si-based solar cell efficiency. Proceedings of SPIE, 2011, , .	0.8	2
47	Laser and thermal properties of Nd:YGd2Sc2Al2GaO12garnet ceramic. Laser Physics Letters, 2012, 9, 697-703.	1.4	2
48	Rare-earth-activated glass-ceramic waveguides: ideal systems for photonics. SPIE Newsroom, 0, , .	0.1	2
49	Fabrication, assessment, and application of confined structures in photonic glasses. , 2009, , .		1
50	X-ray photoelectron spectroscopy of SiO 2 -HfO 2 amorphous and glass-ceramic waveguides: a comparative study. , 2009, , .		1
51	Fabrication and characterization of confined structures for sensing and lasing applications. Proceedings of SPIE, 2010, , .	0.8	1
52	Rare – Earth – Doped Silicate Glass – Ceramic Thin Films for Integrated Optical Devices. Advances in Science and Technology, 0, , .	0.2	1
53	Rare earth doped fluoride glass ceramics: Fabrication of waveguides by PVD and application. , 2009, , .		0
54	Localization of Yb3+, Er3+ and Co2+ Dopants in an Optical Glass Ceramics of MgAl2O4 Spinel Nano-crystals Embedded in SiO2 Glass. NATO Science for Peace and Security Series B: Physics and Biophysics, 2017, , 319-341.	0.3	0